Synchronization of two Rössler systems with switching coupling

Arturo Buscarino, Mattia Frasca, Marco Branciforte, Luigi Fortuna & Julien Clinton Sprott

Nonlinear Dynamics
An International Journal of Nonlinear Dynamics and Chaos in Engineering Systems

ISSN 0924-090X
Volume 88
Number 1

Nonlinear Dyn (2017) 88:673-683
DOI 10.1007/s11071-016-3269-0

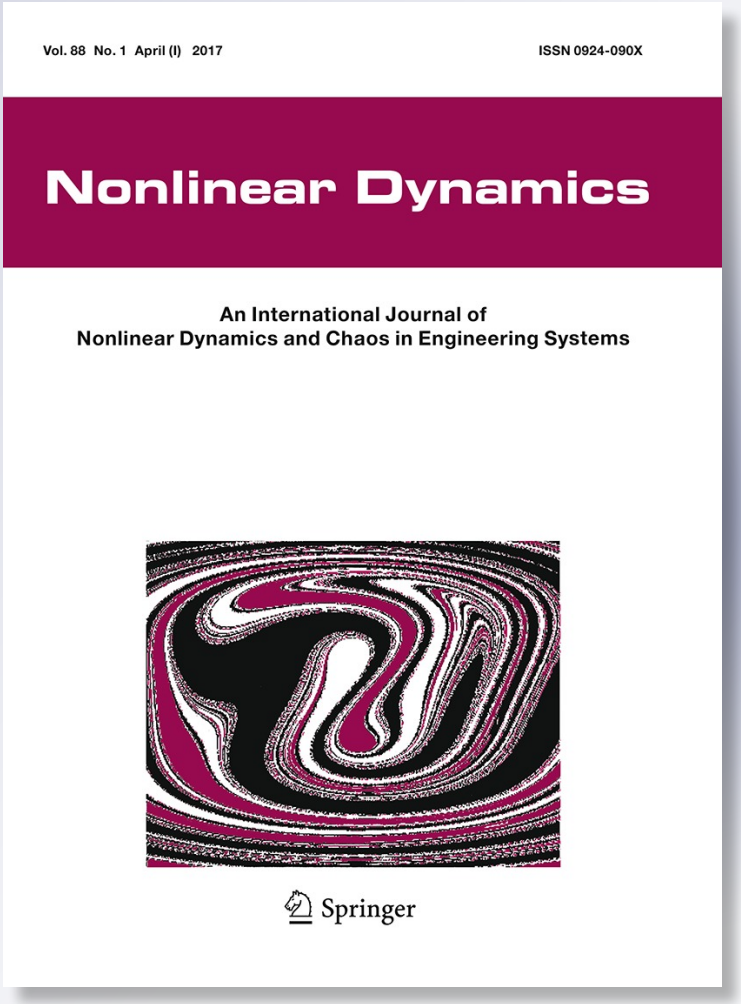

Springer

Nonlinear Dyn (2017) 88:673–683
DOI 10.1007/s11071-016-3269-0

ORIGINAL PAPER

Synchronization of two Rössler systems with switching coupling

Arturo Buscarino · Mattia Frasca · Marco Branciforte · Luigi Fortuna · Julien Clinton Sprott

Received: 30 June 2016 / Accepted: 5 December 2016 / Published online: 20 December 2016

Abstract In this paper, we study a system of two Rössler oscillators coupled through a time-varying link, periodically switching between two values. We analyze the system behavior with respect to the switching frequency. By applying an averaging technique under the hypothesis of high switching frequency, we find that, although each value of the coupling is not suitable for synchronization, switching between the two at a high frequency makes synchronization possible. However, we also find windows of synchronization below the value predicted by this technique, and we develop a master stability function to explain the appearance of these windows. The spectral properties of the system provide a useful tool for understanding the dynamics and synchronization failure in some intervals of the switching frequency. An experimental setup based on a digital/analog circuit is also presented showing experimental results which are in good agreement with the numerical analysis presented.

Keywords Nonlinear dynamics and chaos · Time-varying coupling · Synchronization · Nonlinear circuits

A. Buscarino (✉) · M. Frasca · L. Fortuna
Dipartimento di Ingegneria Elettrica Elettronica e Informatica, Università degli Studi di Catania, Viale A. Doria 6, 95125 Catania, Italy
e-mail: arturo.buscarino@dieei.unict.it

M. Frasca
e-mail: mattia.frasca@dieei.unict.it

L. Fortuna
e-mail: luigi.fortuna@dieei.unict.it

M. Branciforte
ST Microelectronics, Stradale Primosole 50, 95121 Catania, Italy
e-mail: marco.branciforte@st.com

J. C. Sprott
Department of Physics, University of Wisconsin – Madison, Madison, WI 53706, USA
e-mail: csprott@wisc.edu

1 Introduction

The interaction of two nonlinear (in particular, chaotic) systems via coupling typically leads to a variety of significant behaviors, one of the most intriguing of which is synchronization, that is, the coordination of a particular dynamical property of their motion [1]. The type of interaction, its strength, the variables involved in the coupling, and the eventual presence of a delay, produce different coordinated dynamical properties leading to different types of synchronization. The most common forms are complete synchronization in which the two dynamical units evolve following exactly the same trajectory, phase synchronization [2,3] when the coordinated property is the phase, lag synchronization [4] when both amplitudes and phases are locked but with a permanent time lag, and generalized synchronization [5] when a given function of the output of two systems is synchronized. The phenomenon is even more varied when more than two units interact according to a pattern of connectivity through which they share informa-

tion on their current state. Complete synchronization [6], phase synchronization [7], cluster synchronization [8], partial synchronization [9], chimera states [10,11], relay synchronization [12], and remote synchronization [13] are examples of the behaviors observed in a network of coupled oscillators. For complete synchronization of continuous-time identical systems under static coupling, the necessary conditions for the onset of synchronization are derived in [14]. These conditions in many cases can be also considered sufficient for synchronization. Other approaches for the study of the stability of synchronization are based on the definition of Lyapunov functions to assess the sufficient conditions for global synchronization [15]; from another perspective in [16] necessary and sufficient conditions on the boundedness of the derivatives of the vector fields are introduced leading to the design of a distributed control law to obtain local exponential synchronization.

Although the connectivity among the dynamical units is usually considered time-invariant, interaction among dynamical systems may also occur in a discontinuous way (for instance, when it is mediated by links activated according to the relative distance of mobile units [17–19]) or when weights vary in time as the result of an adaptation law [20–22]. In such cases, a key factor in determining the global behavior of the system is the interplay between the timescales, one related to dynamics of the units, and the other defining the rate of variation in the strength of the links. Another important ingredient is the dynamical rule for the variation of the coupling, which may be either a stochastic/periodic activation/deactivation [23,24] or a deterministic law [25]. Both possibilities were explored in early experimental works on two coupled Chua's circuits [26,27]. In particular, in [26] adaptive coupling was used to design communication channels able to compensate for parameter changes, while in [27] it was demonstrated that in a synchronization scheme where two Chua's circuits are pulse coupled, the switching frequency has to be larger than a threshold value to attain synchronization.

This behavior is now grounded on recent theoretical results in the framework of blinking networks [28,29], proving that under the assumption (referred to as the fast switching hypothesis, FSH), that the link changes occur faster *enough* than the oscillator dynamics, the time-varying coupling can be studied by means of the time-average of the coupling matrix. However, establishing when the "*fast enough*" hypothesis holds is still an open issue, so that procedures to determine explicit bounds for the timescale of the process driving the coupling mechanism are currently under investigation [25]. On the other hand, there is evidence that even below the threshold given by the FSH, many interesting phenomena may occur. For instance, a recent study on synchronization of chaotic oscillators coupled via an on–off stochastic network has unveiled the non-trivial existence of windows of complete synchronization for switching frequencies below the predicted lower bound for which the FHS holds [30]. The effects of discontinuous coupling have been also considered in [31–33]. In [31] the role of the on–off rate on synchronization is analyzed, while in [32] the cost of synchronization is studied with respect to the on–off rate of the coupling switching for a given period. A different strategy for discontinuous coupling is addressed in [33], in which coupling is activated only when the trajectory of the considered system visits a specific region in the state-space.

Here we investigate a case study of two Rössler systems interacting through switching coupling and show the presence of interesting phenomena in a regime not dominated by fast switching. We consider the case where the two chaotic systems are coupled through a link whose weight is time-varying, i.e., the weight switches between two fixed values with a given switching frequency. We fix the values so that neither of them can ensure synchronization in the case of static coupling. Despite this, the switching between these two values gives rise to a synchronous behavior. The stability of the synchronization manifold is then studied with respect to the switching frequency, spanning the slow to fast switching regimes, unveiling the close relationship between the two timescales. We remark that the framework proposed in this paper sensibly differs from those considered in [25,31,32]. In fact, instead of activating stochastically each link with probability p as in [25], links are here activated/deactivated with a deterministic switching periodic signal. As concerns [31,32], both papers address the case of an on–off switching in which in the on phase a topology guaranteeing complete synchronization in the static case is considered and discuss the role of the duty cycle of the switching signal, i.e., the duration of the on phase with respect to the off phase, for a fixed frequency. In our paper, instead we consider either topologies for which synchronization in the static case is possible or topologies not guaranteeing synchronization. Furthermore, in our paper the role

of the switching frequency is investigated allowing us to link the dynamical behaviors observed in the region below fast switching with the intrinsic dynamical properties of the Rössler attractor of the single unit.

We also provide an experimental validation of the observed results based on a hybrid platform where the two analog circuits are coupled by digitally controlled links. The use of circuit implementations allows to experimentally verify the numerical evidences gained on the effect of the switching frequency on the synchronization in a more general scenario which includes physical and realistic systems [34]. In realistic systems, in fact, system parameters are always subjected to uncertainties which introduce sensible differences with the corresponding ideal values. Under these conditions, complete synchronization cannot be retrieved and weaker forms of synchronization arise, such as partial synchronization [35,36]. On the other hand, the evaluation of partial synchronization can be exploited in order to estimate unknown parameter values [37,38].

The rest of the paper is organized as follows: in Sect. 2 the model analyzed is described; in Sect. 3 numerical results showing the effects of the switching frequency are reported, and in Sect. 4 the analysis with respect to the switching frequency is presented, while Sect. 5 deals with the experimental validation of the results. Section 6 provides conclusions.

2 Model

The Rössler oscillator is described by the following nonlinear dynamical equations [39]:

$$\begin{aligned} \dot{x} &= -y - z \\ \dot{y} &= x + ay \\ \dot{z} &= b + z(x - c) \end{aligned} \tag{1}$$

where a, b, and c are system parameters. We fix $a = b = 0.2$ and $c = 7$ throughout the rest of the paper so that a chaotic attractor is obtained in the range of considered initial conditions.

We first consider two identical Rössler systems coupled through a diffusive coupling constant in time and acting between the x variables and briefly discuss the behavior of this configuration in view of the application of the fast switching approach. The equations governing the two coupled systems are written as

$$\begin{aligned} \dot{x}_1 &= -y_1 - z_1 + \kappa(x_2 - x_1) \\ \dot{y}_1 &= x_1 + ay_1 \\ \dot{z}_1 &= b + z_1(x_1 - c) \\ \dot{x}_2 &= -y_2 - z_2 + \kappa(x_1 - x_2) \\ \dot{y}_2 &= x_2 + ay_2 \\ \dot{z}_2 &= b + z_2(x_2 - c) \end{aligned} \tag{2}$$

where the subscripts indicate the two paired systems, and κ is the coupling strength. We indicate the state vectors of the two systems as $\mathbf{x}_1 = [\,x_1\ y_1\ z_1\,]^{\mathrm{T}}$ and $\mathbf{x}_2 = [\,x_2\ y_2\ z_2\,]^{\mathrm{T}}$, respectively, and rewrite Eq. (2) in a compact form as

$$\begin{aligned} \dot{\mathbf{x}}_1 &= f(\mathbf{x}_1) + \kappa \mathrm{E}(\mathbf{x}_2 - \mathbf{x}_1) \\ \dot{\mathbf{x}}_2 &= f(\mathbf{x}_2) + \kappa \mathrm{E}(\mathbf{x}_1 - \mathbf{x}_2) \end{aligned} \tag{3}$$

with $\mathrm{E} = \begin{bmatrix} 1 & 0 & 0 \\ 0 & 0 & 0 \\ 0 & 0 & 0 \end{bmatrix}$. Complete synchronization is formally defined as

$$\|\mathbf{x}_1 - \mathbf{x}_2\| \to 0, \quad \mathrm{as} \quad t \to \infty \tag{4}$$

where $\|\cdot\|$ stands for the Euclidean norm. To derive the conditions on κ for complete synchronization, we define the error as $\mathbf{e}(t) = \mathbf{x}_1 - \mathbf{x}_2$ and calculate the error dynamics from Eq. (3):

$$\frac{\mathrm{d}(\mathbf{x}_1 - \mathbf{x}_2)}{\mathrm{d}t} = f(\mathbf{x}_1) - f(\mathbf{x}_2) - s\kappa \mathrm{E}(\mathbf{x}_1 - \mathbf{x}_2) \tag{5}$$

By linearizing around the common solution $\mathbf{x}_1 = \mathbf{x}_2 = \mathbf{s}$, we obtain:

$$\frac{\mathrm{d}\mathbf{e}}{\mathrm{d}t} = \left(\frac{\partial f(\mathbf{x})}{\partial \mathbf{x}}\bigg|_{\mathbf{x}=\mathbf{s}} - 2\kappa \mathrm{E} \right) \mathbf{e} \tag{6}$$

The maximum Lyapunov exponent $\Lambda_{\max}(\kappa)$ for Eq. (6) calculated as a function of κ indicates the region of local stability of the error dynamics, and so of complete synchronization. For this reason, following the terminology of [14], we refer to it as the master stability function (MSF) of the system. In particular, synchronization requires that $\Lambda_{\max}(\kappa) < 0$. Figure 1 displays the MSF for the static coupling case (Eq. (2)). Note that $\Lambda_{\max}(\kappa)$ is negative only in the interval $0.1 < \kappa < 2.35$. This behavior, referred to as class-III MSF [40], is characteristic of a class of systems including the Rössler oscillator with coupling through the variable x.

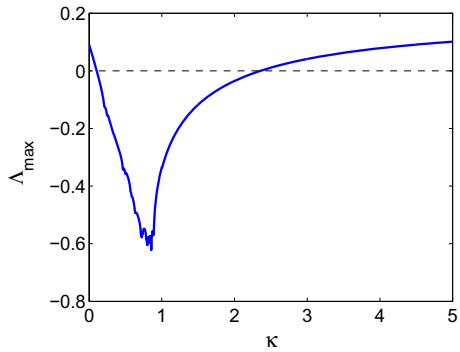

Fig. 1 Master stability function for the system in Eq. (2) with static coupling

We now consider the main object of our study, which is a system formed by two units coupled with a time-varying link given by

$$\begin{aligned}
\dot{x}_1 &= -y_1 - z_1 + \kappa(t)(x_2 - x_1)\\
\dot{y}_1 &= x_1 + a y_1\\
\dot{z}_1 &= b + z_1(x_1 - c)\\
\dot{x}_2 &= -y_2 - z_2 + \kappa(t)(x_1 - x_2)\\
\dot{y}_2 &= x_2 + a y_2\\
\dot{z}_2 &= b + z_2(x_2 - c)
\end{aligned} \tag{7}$$

where the coupling strength $\kappa(t)$ is now a function of time. We assume $\kappa(t) = k_1 + \frac{k_2 - k_1}{2}(\mathrm{sgn}(\cos(\omega t)) + 1)$, with $\mathrm{sgn}(x) = 1$ if $x > 0$ and $\mathrm{sgn}(x) = -1$ otherwise, so that the effective coupling switches between two constant values k_1 and k_2 at a frequency ω. We refer to Eq. (7) as the switching system and analyze its behavior with respect to the switching frequency ω, which is an important bifurcation parameter.

In particular, we select k_1 and k_2 such that neither of the two falls within the synchronization range for the static coupling case (MSF of Fig. 1), that is, $\Lambda_{\max}(k_1) > 0$ and $\Lambda_{\max}(k_2) > 0$. Under these conditions, the problem of synchronization of the switching system is not trivial since the system switches between two configurations that are not synchronizable. A recently developed approach for blinking systems [25] provides a useful tool for understanding the behavior of the system under the hypothesis that the switching occurs at a sufficiently high frequency. The trajectory of the switching system approaches that of the average system in which the coupling is static and given in our case by $k(t) = \bar{k} = \frac{k_1 + k_2}{2}$. In the following, we focus on the case in which k_1 and k_2 also satisfy the condition $\Lambda_{\max}(\bar{k}) < 0$, that is, the prediction of the fast switching approach is that the switching system at high enough ω does synchronize. We will show that the fast switching approach can be effectively used to predict the behavior of the switching system, but synchronization may also occur at lower frequencies in particular windows of ω.

3 Numerical results

In our numerical simulations, we take $k_1 = 0$ and $k_2 = 2.4$. Both values fall outside the range of synchronization identified by the MSF of Fig. 1, i.e., $\Lambda_{\max}(k_1) > 0$ and $\Lambda_{\max}(k_2) > 0$, while the average value $\bar{k} = 1.2$ lies in the stable region with $\Lambda_{\max}(\bar{k}) < 0$.

We investigate the effect of the switching frequency by fixing all the other parameters and varying ω from 0 to 1.5 (the limiting case $\omega = 0$ corresponds to uncoupled dynamics). For each value of ω, we integrate Eq. (7) using a 4th order Runge–Kutta algorithm with an adaptive step size for $T = 10^7$ and sample the result at $dt = 0.01$, thus giving $M = 10^9$ samples. The normalized average synchronization error $E(\omega)$ is then calculated from

$$E(\omega) = \sum_{h=1}^{M} \frac{\sqrt{(x_1(h)-x_2(h))^2 + (y_1(h)-y_2(h))^2 + (z_1(h)-z_2(h))^2}}{\sqrt{x_1(h)^2 + y_1(h)^2 + z_1(h)^2 + x_2(h)^2 + y_2(h)^2 + z_2(h)^2}} \tag{8}$$

The synchronization error $E(\omega)$ is normalized so that $E = 1$ means that the two trajectories are completely uncorrelated, $E > 1$ indicates anti-correlation, while $E \to 0$ corresponds to the highest correlation.

The synchronization error $E(\omega)$ as shown in Fig. 2 is not a monotonic function of ω. For $\omega > 1.3$, the

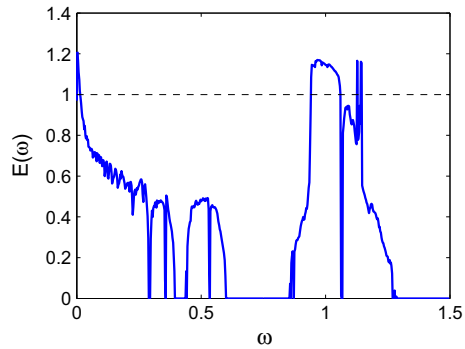

Fig. 2 Average synchronization error $E(\omega)$ with respect to the switching frequency ω

system is synchronized. Therefore, we conclude that $\omega \simeq 1.3$ represents the boundary between the region in which the FSH holds, and that in which the frequency of the switching is not "fast enough". For $\omega > 1.3$, the effect of the time-varying connectivity, evolving with a timescale high enough with respect to the Rössler dynamics, is equivalent to driving the system with a constant coupling coefficient, which is the average of the two coupling strengths k_1 and k_2. The two oscillators, in fact, are always synchronized and chaotic as shown in Fig. 3.

The behavior at low frequencies ($\omega < 0.2$) is somewhat expected from the choice of k_1 and k_2. In this case, the system slowly alternates between two configurations, which are both not synchronizable, and the global behavior is unsynchronized.

The most interesting frequencies are between the regions of slow and fast switching, $\omega \in [0.2, 1.3]$, where windows of synchronization and unsynchronized behavior alternate. Even when the FSH does not hold, i.e., when the dynamics of the link activation has timescales comparable to those of the Rössler system, there is the possibility of complete synchronization.

Starting from the boundary with the region where FSH holds and decreasing the switching frequency, we examine the behavior of the two Rössler oscillators as a function of ω. Below $\omega = 1.3$, a large window ($0.9 < \omega < 1.3$) of unsynchronized motion is found. The system attractor is significantly different from the attractor for a single Rössler oscillator. For example, Fig. 4 shows the chaotic attractor corresponding to $\omega = 1.0$. We also observe two other dynamical behav-

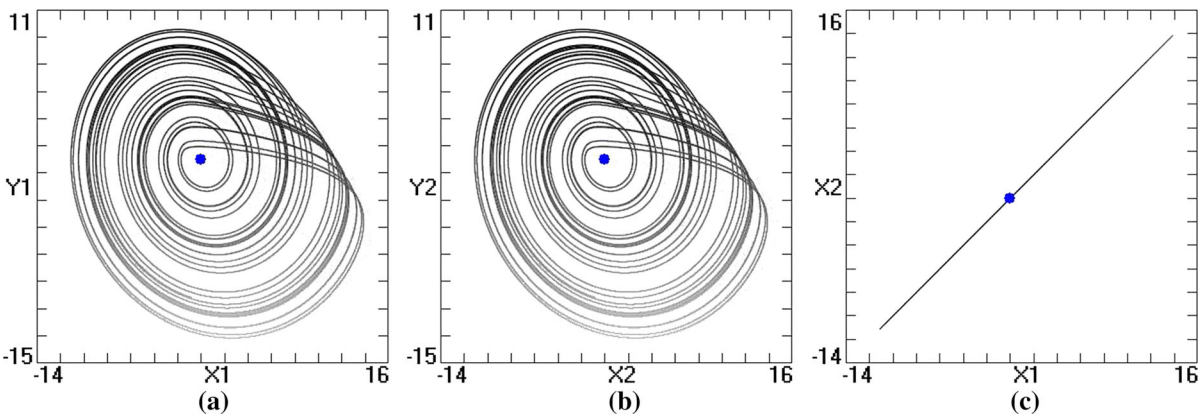

Fig. 3 Complete synchronization of two Rössler oscillators coupled by a switching signal with $\omega = 1.5$. Projection of the attractor on the planes **a** $x_1 - y_1$, **b** $x_2 - y_2$, **c** $x_1 - x_2$

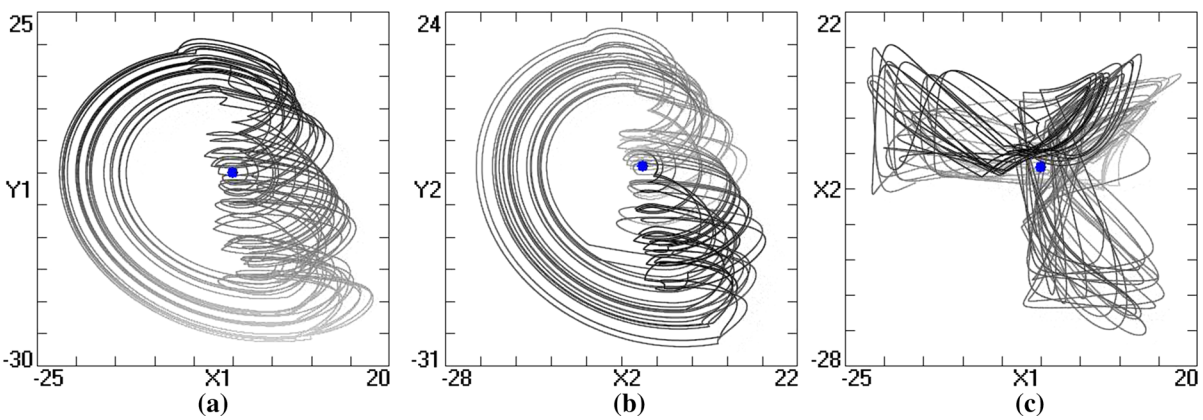

Fig. 4 Unsynchronized motion of two Rössler oscillators coupled by a switching signal with $\omega = 1$. Projection of the attractor on the planes **a** $x_1 - y_1$, **b** $x_2 - y_2$, **c** $x_1 - x_2$

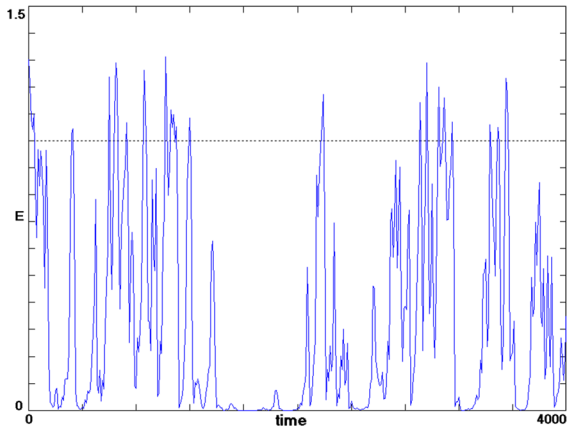

Fig. 5 Temporal evolution of the average synchronization error E for $\omega = 1.13$ showing intermittency

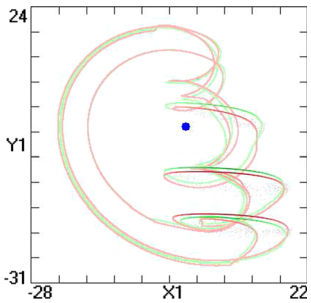

Fig. 6 Limit cycles in the two Rössler oscillators coupled by a switching signal with $\omega = 0.9656$. Projection of the two attractors on the plane $x - y$

iors. At $\omega \approx 0.97$ and $\omega \approx 1.13$, which correspond to values immediately before and after the unsynchronized window $0.9 < \omega < 1.3$, intermittency between synchronous and unsynchronous motion occurs. The intermittency is evident in the error E in Fig. 5. The attractor for this case also alternates between the original Rössler chaotic attractor (obtained when the synchronization error is close to zero) and the one shown in Fig. 4, obtained when the error is larger. Furthermore, at $\omega \approx 0.9656$ two stable limit cycles coexist as shown in Fig 6.

For a further decrease in the switching frequency, a new window of synchronization occurs at $0.6 < \omega < 0.9$. Below $\omega = 0.6$ a series of unsynchronized/synchronized windows are seen, whose widths decrease with decreasing ω. Within all the windows, including the main around $\omega = 1$, a narrow range of synchronization is observed.

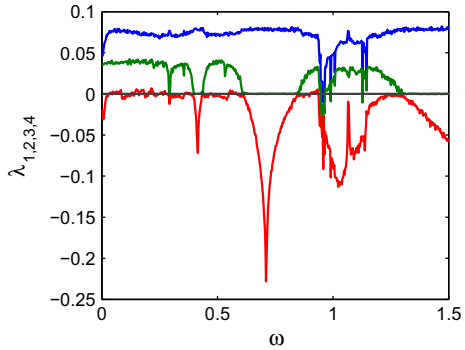

Fig. 7 The four largest Lyapunov exponents for the system in Eq. (7)

The observed behavior is confirmed by analysis of the Lyapunov spectrum of system (7). The four largest Lyapunov exponents are shown in Fig. 7. Regions of synchronization have one positive Lyapunov exponent, while the unsynchronized regions have two positive Lyapunov exponents corresponding to hyperchaos in the six-dimensional system. The sign of the second largest nonzero Lyapunov exponent thus confirms the windows of synchronous and unsynchronous motion found from the synchronization error.

4 Analysis

From the previous numerical results, it appears that the switching frequency provides a bifurcation parameter, especially when the FSH does not hold, that is, when the switching rate is comparable to the dynamics of the Rössler system. The switching frequency affects not only the synchronization, but also the dynamics of the attractors. In this section, we investigate the power spectra of the Rössler state variables and correlate them with the windows observed in Figs. 2 and 7, and then we develop a MSF for the case of two oscillators with time-varying coupling.

We begin by observing that the power spectral density of an uncoupled Rössler system (1) as shown in Fig. 8 is characterized by a strong dominant component, corresponding to the large oscillations in the $x-y$ plane, and located at a frequency $\omega_s \simeq 1.067$. The large window of unsynchronized behavior in Fig. 2 at the boundary with the fast switching region is around this frequency. A closer inspection of the spectrum of the switching system shows that in this window a resonance

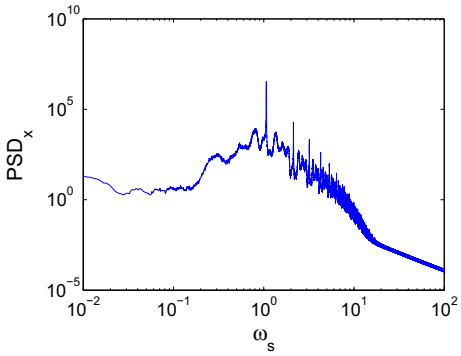

Fig. 8 Power spectral density for the x variable of the Rössler system in Eq (1)

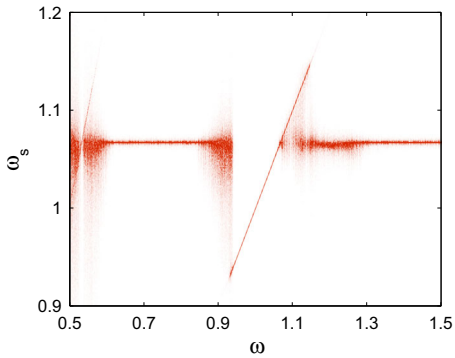

Fig. 9 Power spectral density for the x variable of the Rössler system in Eq (7), for different values of ω. *Red* indicates higher power. (Color figure online)

effect occurs as shown in the spectrogram in Fig. 9. The figure shows the power spectral density (color coded) for the spectrum components, indicated as ω_s, between 0.9 and 1.2 and for different values of the switching frequency $\omega \in [0.5, 1.5]$. In the two windows where the two systems are synchronized (one is the fast switching region for higher values of ω, and the other is the window $0.6 < \omega < 0.9$), the dominant frequency is ω_R, the same as for the uncoupled Rössler system, that is, when the two systems synchronize, they evolve following the chaotic trajectory $\mathbf{s}$ of the uncoupled system. On the contrary, when the coupling strength switches at a frequency ω comparable to ω_R, in particular in the window $0.95 < \omega < 1.15$, the dominant frequency is locked to the switching frequency, thus resulting in a strong modification of the dominant frequency with respect to the uncoupled case. This explains the different shape of the attractor in this range (Fig. 4). Furthermore, a similar effect is observed at the first subharmonic of the dominant frequency around $\omega = 0.5335$ superposed on the window of unsynchronized behavior. Presumably, the same locking occurs in narrower ranges around all the other subharmonics.

From a different perspective, a similar conclusion can be derived starting from the Lur'e form of the Rössler system [41]. A nonlinear dynamical system can be represented in Lur'e form if it is possible to decompose it in two parts: a linear system and a feedback nonlinear part. In [41] the Lur'e representation of the Rössler is given, leading to a linear part $G(s) = \frac{1}{s^3+(c-a)s^2+(1-ca)s+c} = \frac{1}{s^3+6.8s^2-0.4s+7}$. The two unstable poles of $G(s)$ are a complex conjugate pair yielding a resonance peak located at $1 rad/s$. Since the coupling term acts as an external input provided to the linear part of the system, if it contains a strong component around the resonance peak, it is going to be strongly amplified: this corresponds to increase the effective coupling strength outside the allowed range and may qualitatively explain the loss of synchronization obtained for $\omega \approx 1$.

We now derive a MSF for the time-varying coupling. To do this, we consider system (7) and calculate the error dynamics and linearize around the common solution $\mathbf{x}_1 = \mathbf{x}_2 = \mathbf{s}$ to obtain

$$\frac{d(\mathbf{e})}{dt} = \left(\frac{\partial f(\mathbf{x})}{\partial \mathbf{x}}\bigg|_{\mathbf{x}=\mathbf{s}} - 2\kappa(t)\mathrm{E} \right) \mathbf{e} \tag{9}$$

with $\kappa(t) = k_1 + \frac{k_2-k_1}{2}(\mathrm{sgn}(\cos(\omega t)) + 1)$. Figure 10 shows the maximum Lyapunov exponent $\Lambda_{\max}(\omega)$ as a function of ω for Eq. (9). Values of ω such that $\Lambda_{\max}(\omega) < 0$ synchronize the pair of Rössler oscillators, while $\Lambda_{\max}(\omega) > 0$ indicates that the error does not decay to zero for that value of the switching frequency. The curve $\Lambda_{\max}(\omega)$ versus ω perfectly explains the presence of several windows of synchronization and unsynchronized motion for system (7).

We next calculate the maximum Lyapunov exponent $\Lambda_{\max}(\omega, k_2)$ for the system in Eq. (9) with time-varying coupling as a function of the two parameters ω and k_2. In Fig. 11 the regions of the parameter space $k_2 - \omega$ in which $\Lambda_{\max}(\omega, k_2) \leq 0$ ($\Lambda_{\max}(\omega, k_2) > 0$) are reported in light blue (red). It clearly appears that different windows of unsynchronized behavior fixing k_2 and varying ω can be observed for a large range of k_2. Furthermore, a novel behavior is enlightened when ω is fixed and k_2 varied. The static MSF of the x-

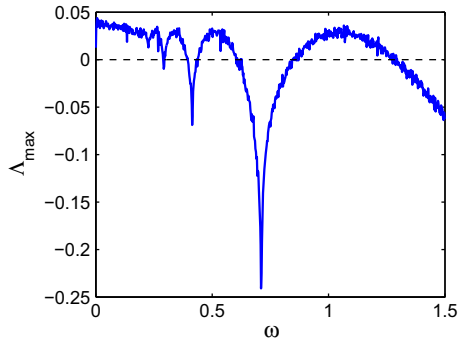

Fig. 10 Maximum Lyapunov exponent $\Lambda_{\max}(\omega)$ for the system in Eq. (9) with time-varying coupling. $k_1 = 0$, $k_2 = 2.2$

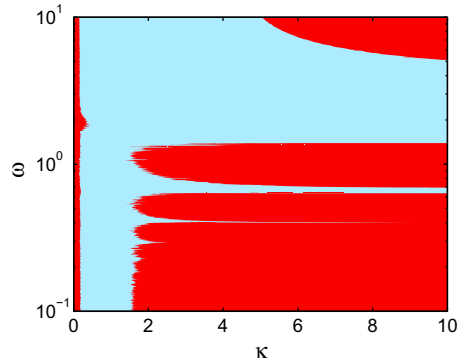

Fig. 11 Regions in the parameter space ω versus κ where the maximum Lyapunov exponent $\Lambda_{\max}(\omega, k_2)$ is positive (*red region*) or negative (*blue region*) for the system in Eq. (9) with time-varying coupling. (Color figure online)

coupled Rössler oscillator, as it can be seen from Fig. 1, is classified as class-III, i.e., synchronization manifold is stable only in a given interval of the coupling factor. This behavior can be retrieved when switching is fast with respect to the system dynamics, i.e., $\omega \geq 10 rad/s$. However, when switching frequency is below this threshold, the MSF appears as class-II, i.e., synchronization is preserved for all values of the coupling factor above a single threshold. This behavior is found several times decreasing ω between two subsequent resonance peaks.

We mention here that other chaotic dynamics can be considered. When coupling two Lorenz systems with an on–off coupling through the z variable, in fact, the synchronization range in terms of the coupling strength is widened with respect to the static case, but, unlike the Rössler systems, remains limited between two values.

5 Experimental investigation

In this section, the system of two Rössler oscillators with switching coupling is investigated experimentally using an electronic circuit governed by Eq. (7). Each Rössler oscillator was implemented using the electrical scheme [42]. The timescale of the circuit was rescaled by a factor $K \approx 2100$ so that the circuit waveforms exactly correspond to those of the Rössler system (1).

Unlike static coupling, which can be realized by means of a single resistor between the capacitors associated with the corresponding state variables, coupling in the experimental setup used a pulse-width-modulated (PWM) analog switch in series with a coupling resistor. This strategy facilitates extending the setup to a network of switched connections. We also explored solutions based on a digital resistor, but the resolution provided by off-the-shelf digital resistors both in terms of values and switching time was found inadequate for our purpose.

The coupling scheme was implemented using two components: the analog switch ADG452 and the ST microcontroller unit (MCU) STM32F303VCT6 for the generation and control of the PWM signal. The ADG452 embeds four independently selectable bi-directional switches, has a low on-resistance (on the order of 5Ω), fast switching times ($t_{ON} = 70ns$, $t_{OFF} = 60ns$), and is TTL-/CMOS-compatible. The microcontroller STM32F303VCT6 is an ARM-based Cortex-M4, 32bit microcontroller with an embedded floating point unit. It has a core clock up to 72 MHz, a 256 kB Flash memory, 48 kB SRAM, and a wide range of peripherals such as analog-to-digital and digital-to-analog converters, timers, and direct memory access. It requires a voltage supply in the range of 2.0 to 3.6 V.

The value of the coupling resistor is controlled by the duty cycle (DC) of the PWM signal driving the analog switch. Turning the switch on and off has the effect of multiplying the fixed coupling resistor by a factor inversely proportional to the DC according to the relationship

$$R_{\text{eq}} = \frac{100}{\text{DC}} R_c \tag{10}$$

The ADG452 was controlled with a 40-kHz PWM, which is adequate since the frequency range of the Rössler system is below 5 kHz. Although this solution can switch between two nonzero values of the

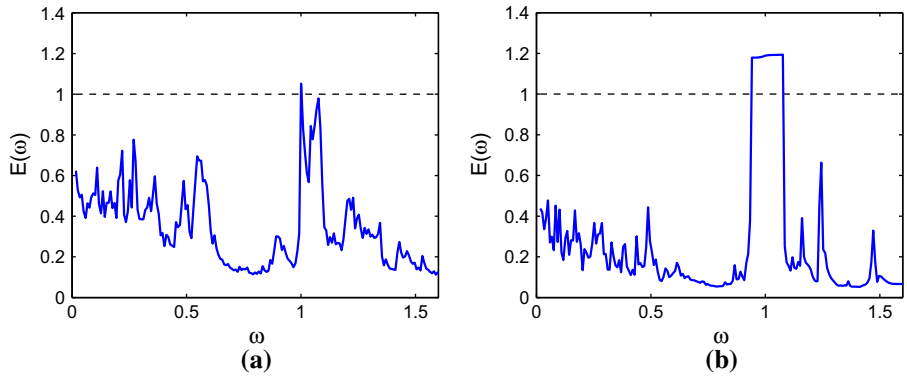

Fig. 12 Average normalized error $E(\omega)$ calculated on **a** data acquired from the experimental system and **b** data obtained from numerical integration of the identified model of the implemented circuit. The frequency axis in (**a**) is rescaled by a factor K to allow comparison with numerical results

coupling resistance, it allows low values of the coupling ($k_1 = 0.02$), which adequately approximate two disconnected circuits.

The waveforms corresponding to the six state variables were acquired using an NI-USB6255 data acquisition board at a sampling frequency of $f_s = 80\,\text{kHz}$ and post-processed to compute the average normalized error $E(\Omega)$ as in Eq. (8), where $\Omega = K\omega$ is the switching frequency in the rescaled circuit.

Figure 12a shows the trend of $E(\Omega)$. To facilitate comparison with numerical results, the frequency axis has been rescaled in terms of the variable ω. The predicted peak of desynchronization around $\omega = 1.00$ is confirmed in the experiment. Due to component tolerances, complete synchronization ($E = 0$) is not obtained, but practical synchronization [43,44] ($E < 0.2$) is observed. To better compare the experimental results with numerical simulations, these have to explicitly take into account in the model the component tolerances. To this aim, the parameters actually implemented in the circuit were identified using a symbolic regression algorithm [45]. The results obtained from the model including tolerances are shown in Fig. 12(b). The results are in agreement with those discussed in [36] in which an error bound is derived in presence of differences between coupled circuits as a function of largest transverse Lyapunov exponent. For our case, taking into account an uncertainty in parameter values of the 1% and, applying the methods for error bound evaluation presented in [36], we obtain a predicted bound for the error of 0.56, which is above the effective error retrieved in the experiment. The windows of practical synchronization are in good agreement with those predicted by the model, demonstrating the robustness of the observed phenomena.

6 Conclusions

In this paper, two Rössler oscillators coupled through a time-varying link were investigated. In particular, the coupling strength is periodically switched between two values. The observed behavior is significantly richer than the case of other chaotic circuits such as two coupled Chua's circuits, for which there is only a single transition frequency between synchronization and unsynchronous motion [27].

Although each of the two coupling values precludes synchronization when statically applied to the system, switching between them may result in stabilizing the synchronization manifold. This occurs not only at high switching frequencies as predicted by fast switching theory, but also in several windows at lower values of the frequency.

We have shown that the alternation of windows of synchronization and unsynchronized motion can be explained in terms of a MSF illustrating the behavior of the maximum Lyapunov exponent transverse to the synchronization manifold as a function of the switching frequency. Windows of synchronization correspond to negative values of the maximum transverse Lyapunov exponent, while unsynchronized behavior is obtained when this quantity is positive.

The study of time-varying coupling is motivated by real-life examples of complex systems in which the topology of connections between units evolves following its own dynamics. In particular, the on–off mechanism of the coupling allows to obtain a non-trivial behavior, i.e., the range of the coupling coefficient in which synchronization is achieved becomes infinite for a large set of the switching frequency. This allows to design adaptive strategies through which the switching

frequency can be set according to specific constraints on the coupling strength.

Although the phenomenon of the appearance of windows of synchronization beyond the regime of fast switching has been recently reported in other works [30–32], in this paper we have linked it to the effects of the coupling on the dynamical properties of the unit. We have, in fact, highlighted a strong effect of the switching coupling on the spectral properties of the two oscillators, since, for a switching frequency close to the dominant component of the spectrum of the isolated Rössler oscillators, the dominant component locks to the switching frequency, resulting in a significant change of the chaotic dynamics and a failure of synchronization.

Hence the spectral properties of the system and analysis of the MSF derived for the time-varying coupling allow one to predict the regions of synchronizability beyond that expected from fast switching analysis. An interesting behavior occurs for switching frequencies below the fast switching, where the synchronization interval, typical of class-III MSF, is enlarged toward infinity. These regions agree well with the results of numerical and experimental analysis.

Acknowledgements We acknowledge Fabrizio La Rosa for help in realizing the experimental setup.

References

1. Boccaletti, S., Kurths, J., Osipov, G., Valladares, D.L., Zhou, C.S.: The synchronization of chaotic systems. Phys. Rep. **366**, 1–101 (2002)
2. Rosenblum, M.G., Pikovsky, A.S., Kurths, J.: Phase synchronization of chaotic oscillators. Phys. Rev. Lett. **76**, 1804–1807 (1996)
3. Rosa, E.R., Ott, E., Hess, M.H.: Transition to phase synchronization of chaos. Phys. Rev. Lett. **80**, 1642–1645 (1998)
4. Rosenblum, M.G., Pikovsky, A.S., Kurths, J.: From phase to lag synchronization in coupled chaotic oscillators. Phys. Rev. Lett. **78**, 4193–4196 (1997)
5. Rulkov, N.F., Sushchik, M.M., Tsimring, L.S., Abarbanel, H.D.I.: Generalized synchronization of chaos in directionally coupled chaotic systems. Phys. Rev. E **51**, 980–994 (1995)
6. Gomez-Gardenes, J., Moreno, Y., Arenas, A.: Paths to synchronization on complex networks. Phys. Rev. Lett. **98**, 034101-1–034101-4 (2007)
7. Arenas, A., Diaz-Guilera, A., Kurths, J., Moreno, Y., Zhou, C.: Synchronization in complex networks. Phys. Rep. **469**, 93–153 (2008)
8. Pecora, L.M., Sorrentino, F., Hagerstrom, A.M., Murphy, T.E., Roy, R.: Cluster synchronization and isolated desynchronization in complex networks with symmetries. Nat. Commun. **5**, 4079-1–4079-8 (2014)
9. Wickramasinghe, M., Kiss, I.Z.: Spatially organized partial synchronization through the chimera mechanism in a network of electrochemical reactions. Phys. Chem. Chem. Phys. **16**, 18360–18369 (2014)
10. Abrams, D.M., Strogatz, S.H.: Chimera states for coupled oscillators. Phys. Rev. Lett. **93**, 174102-1–174102-4 (2004)
11. Gambuzza, L.V., Buscarino, A., Chessari, S., Fortuna, L., Meucci, R., Frasca, M.: Experimental investigation of chimera states with quiescent and synchronous domains in coupled electronic oscillators. Phys. Rev. E **90**, 032905-1–032905-8 (2014)
12. Gutierrez, R., Sevilla-Escoboza, R., Piedrahita, P., Finke, C., Feudel, U., Buldú, J.M., Huerta-Cuellar, G., Jaimes-Reategui, R., Moreno, Y., Boccaletti, S.: Generalized synchronization in relay systems with instantaneous coupling. Phys. Rev. E **88**, 052908-1–052908-5 (2013)
13. Gambuzza, L.V., Cardillo, A., Fiasconaro, A., Fortuna, L., Gmez-Gardees, J., Frasca, M.: Analysis of remote synchronization in complex networks. Chaos **23**, 043103-1–043103-8 (2013)
14. Pecora, L.M., Carroll, T.L.: Master stability functions for synchronized coupled systems. Phys. Rev. Lett. **80**, 2109–2112 (1998)
15. Wu, X., Gui, Z., Lin, Q., Cai, J.: A new Lyapunov approach for global synchronization of non-autonomous chaotic systems. Nonlinear Dyn. **59**, 427–432 (2010)
16. Andrieu, V., Jayawardhana, B., Tarbouriech, S.: Necessary and sufficient condition for local exponential synchronization of nonlinear systems. In: Proceedings of the 2015 IEEE 54th Annual Conference on Decision and Control (CDC), pp. 2981–2986 (2015)
17. Frasca, M., Buscarino, A., Rizzo, A., Fortuna, L.: Synchronization of moving chaotic agents. Phys. Rev. Lett. **100**, 044102-1–044102-4 (2008)
18. Frasca, M., Buscarino, A., Rizzo, A., Fortuna, L.: Spatial pinning control. Phys. Rev. Lett. **108**, 204102-1–204102-5 (2012)
19. Fujiwara, N., Kurths, J., Diaz-Guilera, A.: Synchronization in networks of mobile oscillators. Phys. Rev. E **83**, 025101-1–025101-4 (2011)
20. Yu, W., De Lellis, P., Chen, G., Di Bernardo, M., Kurths, J.: Distributed adaptive control of synchronization in complex networks. IEEE Trans. Autom. Control **57**, 2153–2158 (2012)
21. Lehnert, J., Hövel, P., Selivanov, A., Fradkov, A., Schöll, E.: Controlling cluster synchronization by adapting the topology. Phys. Rev. E **90**, 042914-1–042914-8 (2014)
22. Gambuzza, L.V., Buscarino, A., Fortuna, L., Frasca, M.: Memristor-based adaptive coupling for consensus and synchronization. IEEE Trans. Circuits Syst. I Regul. Pap. **62**, 1175–1184 (2015)
23. Belykh, I.V., Belykh, V.N., Hasler, M.: Blinking model and synchronization in small-world networks with a time-varying coupling. Phys. D **195**, 188–206 (2004)
24. Buscarino, A., Frasca, M., Gambuzza, L.V., Hövel, P.: Chimera states in time-varying complex networks. Phys. Rev. E **91**, 022817-1–022817-7 (2015)

25. Hasler, M., Belykh, V.M., Belykh, I.V.: Dynamics of stochastically blinking systems. Part I: finite time properties. SIAM J. Appl. Dyn. Syst. **12**, 1007–1030 (2013)
26. Chua, L.O., Yang, T., Zhong, G.Q., Wu, C.W.: Synchronization of Chua's circuits with time-varying channels and parameters. IEEE Trans. Circuits Syst. I Fundam. Theory Appl. **43**, 862–868 (1996)
27. Fortuna, L., Frasca, M., Rizzo, A.: Experimental pulse synchronisation of two chaotic circuits. Chaos Solitons Fractals **17**, 355–361 (2003)
28. Skufca, J.D., Bollt, E.: Communication and synchronization in disconnected networks with dynamic topology: moving neighborhood networks. Math. Biosci. Eng. **1**(2), 347–359 (2004)
29. Porfiri, M., Stilwell, D.J., Bollt, E.M., Skufca, J.D.: Random talk: random walk and synchronizability in a moving neighborhood network. Phys. D **224**, 102–113 (2006)
30. Jeter, R., Belykh, I.: Synchronization in on-off stochastic networks: windows of opportunity. IEEE Trans. Circuits Syst. I Regul. Pap. **62**, 1260–1269 (2015)
31. Chen, L., Qiu, C., Huang, H.B.: Synchronization with on-off coupling: role of time scales in network dynamics. Phys. Rev. E **79**, 045101-1–045101-4 (2009)
32. Chen, L., Qiu, C., Huang, H.B., Qi, G.X., Wang, H.J.: Facilitated synchronization of complex networks through a discontinuous coupling strategy. Eur. Phys. J. B **76**, 625–635 (2010)
33. Schröder, M., Mannattil, M., Dutta, D., Chakraborty, S., Timme, M.: Transient uncoupling induces synchronization. Phys. Rev. Lett. **115**, 054101-1–054101-5 (2015)
34. Wang, C., He, Y., Ma, J., Huang, L.: Parameters estimation, mixed synchronization, and antisynchronization in chaotic systems. Complexity **20**, 64–73 (2014)
35. Ma, J., Song, X., Jin, W., Wang, C.: Autapse-induced synchronization in a coupled neuronal network. Chaos Solitons Fractals **80**, 31–38 (2015)
36. Illing, L., Brocker, J., Kocarev, L., Parlitz, U., Abarbanel, H.D.I.: When are synchronization errors small? Phys. Rev. E **66**, 036229-1–036229-8 (2002)
37. Ma, J., Li, F., Huang, L., Jin, W.: Complete synchronization, phase synchronization and parameters estimation in a realistic chaotic system. Commun. Nonlinear Sci. Numer. Simul. **16**, 3770–3785 (2011)
38. Li, F., Wang, C., Ma, J.: Reliability of linear coupling synchronization of hyperchaotic systems with unknown parameters. Chin. Phys. B **22**, 100502-1–100502-8 (2013)
39. Rössler, O.E.: An equation for continuous chaos. Phys. Lett. A **57**, 397–398 (1976)
40. Boccaletti, S., Latora, V., Moreno, Y., Chavez, M., Hwang, D.U.: Complex networks: structure and dynamics. Phys. Rep. **424**, 175–208 (2008)
41. Genesio, R., Innocenti, G., Gualdani, F.: A global qualitative view of bifurcations and dynamics in the Rössler system. Phys. Lett. A **372**, 1799–1809 (2008)
42. Buscarino, A., Fortuna, L., Frasca, M., Sciuto, G.: A Concise Guide to Chaotic Electronic Circuits. Springer, Berlin (2014)
43. Buscarino, A., Fortuna, L., Frasca, M.: Experimental robust synchronization of hyperchaotic circuits. Phys. D **238**, 1917–1922 (2009)
44. Montenbruck, J.M., Bürger, M., Allgöwer, F.: Practical synchronization with diffusive couplings. Automatica **53**, 235–243 (2015)
45. Schmidt, M., Lipson, H.: Distilling free-form natural laws from experimental data. Science **324**, 81–85 (2009)